

Prospects for direct dark matter detection in the Constrained MSSM

Roberto Trotta ^a

^a *Astrophysics Department, Oxford University
Denys Wilkinson Building, Keble Road, Oxford OX1 3RH, United Kingdom*

Roberto Ruiz de Austri ^b

^b *Departamento de Física Teórica C-XI and Instituto de Física Teórica C-XVI,
Universidad Autónoma de Madrid, Cantoblanco, 28049 Madrid, Spain*

Leszek Roszkowski ^c

^c *Department of Physics and Astronomy, University of Sheffield,
Sheffield S3 7RH, England*

Abstract

We outline the WIMP dark matter parameter space in the Constrained MSSM by performing a comprehensive statistical analysis that compares with experimental data predicted superpartner masses and other collider observables as well as a cold dark matter abundance. We include uncertainties arising from theoretical approximations as well as from residual experimental errors on relevant Standard Model parameters.

We present high-probability regions for neutralino dark matter direct detection cross section, and we find that $10^{-10} \text{ pb} \lesssim \sigma_p^{SI} \lesssim 10^{-8} \text{ pb}$ for direct WIMP detection (with details slightly dependent on the assumptions made). We highlight a complementarity between LHC and WIMP dark matter searches in exploring the CMSSM parameter space. We conclude that most of the 95% probability region for the cross section will be explored by future one-tonne detectors, that will therefore cover most of the currently favoured region of parameter space.

Key words:
PACS:

1. Introduction

Two of the most challenging questions facing particle physics today are the instability of the Higgs mass against radiative corrections (known as the “fine-tuning problem”) and the nature of dark matter. Unlike the Standard Model (SM), weak scale softly broken supersymmetry (SUSY) provides solutions to both of them. Firstly, the fine-tuning problem is addressed via the cancellation of quadratic divergences in the radiative corrections to the Higgs mass. Secondly, assuming R -parity, the lightest supersymmetric particle (LSP) is a leading weakly interactive massive particle (WIMP) candidate for cold dark matter (CDM). Despite these and other attractive features, without a reference to grand unified theories (GUTs), low energy SUSY models suffer from the lack of predictivity due to a large number of free parameters (*e.g.*, over 120 in the Minimal Supersymmetric Standard Model (MSSM)), most of which

arise from the SUSY breaking sector.

The MSSM with one particularly popular choice of universal boundary conditions at the grand unification scale is called the Constrained Minimal Supersymmetric Standard Model (CMSSM) [1]. The CMSSM is defined in terms of five free parameters: common scalar (m_0), gaugino ($m_{1/2}$) and tri-linear (A_0) mass parameters (all specified at the GUT scale) plus the ratio of Higgs vacuum expectation values $\tan \beta$ and $\text{sign}(\mu)$, where μ is the Higgs/higgsino mass parameter whose square is computed from the conditions of radiative electroweak symmetry breaking (EWSB). The economy of parameters in this scheme makes it a useful tool for exploring SUSY phenomenology.

Many studies have explored the phenomenology of the CMSSM or other SUSY models, mostly by evaluating the goodness-of-fit of points scanned using fixed grids in parameter space, see *e.g.* [2,3,4,5,6,7]. However, this approach has several severe limitations. Firstly, the number

of points required scales as k^N , where N is the number of the model's parameters and k the number of points for each of them. Therefore this approach becomes highly inefficient for exploring with sufficient resolution parameter spaces of even modest dimensionality, say $N > 3$. Secondly, narrow “wedges” and similar features of parameter space can easily be missed by not setting a fine enough resolution (which, on the other hand, may be completely unnecessary outside such special regions). Thirdly, extra sources of uncertainties (*e.g.*, those due to the lack of precise knowledge of SM parameter values) and relevant external information (*e.g.*, about the parameter range) are difficult to accommodate in this scheme.

In this work we report results from a Bayesian exploration of the CMSSM parameter space, obtained through the use of Markov Chain Monte Carlo methods. In particular we focus on the prospects for direct neutralino dark matter detection with the next generation of dark matter searches. We refer the reader to [8] for full details. The Bayesian approach has several technical and statistical advantages over the more traditional fixed-grid scan technique, the most important being perhaps the ability to incorporate all relevant sources of uncertainties, *e.g.* the residual uncertainty in the value of SM parameters. This means that the inferred high probability regions in terms of *e.g.* neutralino mass and scattering cross section take fully into account all sources of uncertainty relevant to the problem. For other works applying a similar approach to the CMSSM, see [9] (with some relevant differences) and more recently [10,11].

2. Parameter space, priors and data used

We restrict our analysis to the case $\text{sign}(\mu) = +1$, as motivated by the fact that the observed anomalous magnetic moment of the muon is positive, and since the sign of the SUSY contribution to it is the same as the sign of μ . We thus consider the 8 dimensional parameter space (θ, ψ) , where θ is a vector of CMSSM parameters,

$$\theta = (m_0, m_{1/2}, A_0, \tan \beta) \quad (1)$$

while ψ is a vector of relevant SM parameters,

$$\psi = (M_t, m_b(m_b)^{\overline{MS}}, \alpha_{\text{em}}(M_Z)^{\overline{MS}}, \alpha_s(M_Z)^{\overline{MS}}), \quad (2)$$

where M_t is the pole top quark mass, $m_b(m_b)^{\overline{MS}}$ is the bottom quark mass at m_b , while $\alpha_{\text{em}}(M_Z)^{\overline{MS}}$ and $\alpha_s(M_Z)^{\overline{MS}}$ are the electromagnetic and the strong coupling constants at the Z pole mass M_Z , the last three evaluated in the \overline{MS} scheme. We are not interested in constraining the value of the SM parameters, but rather in including the effect of the uncertainty in their experimental determination on the mass spectra, cosmological dark matter abundance and other observable quantities. This in turns has a non-negligible impact when making inferences on the high probability regions for the CMSSM parameters, θ , or for any other derived quantity. At the end of the analysis, the

set of so called “nuisance parameters” ψ is integrated out from our probability distribution function (pdf). It turns out that including the nuisance parameters in our analysis as free parameters (rather than fixing them to the central experimental value as it is done in most grid scans) has an important impact in widening the constraints on the CMSSM parameters, an effect that should not be ignored when carrying out proper statistical inference on θ or on other quantities of interest such as the dark matter scattering cross section.

Bayesian statistics makes use of Bayes theorem,

$$p(\eta|d) = \frac{p(d|\eta, f(\eta))\pi(\eta)}{p(d)}. \quad (3)$$

where we have introduced $\eta = (\theta, \psi)$, to compute the posterior probability distribution $p(\eta|d)$. On the rhs of Eq. (3), the quantity $p(d|\eta, f(\eta))$, is called the *likelihood* and it supplies the information provided by the data, by comparing the base parameters η or any derived function $f(\eta)$ to the data d . The quantity $\pi(\eta)$ denotes a *prior probability density function* (hereafter called simply *a prior*) which encodes our state of knowledge about the values of the parameters before we see the data. We take the prior to be flat (*i.e.*, constant) in the variables η , and we further need to specify the range along each direction. If the constraining power of the likelihood is strong enough to override the choice of the prior, then the latter does not matter in the final inference based on the posterior pdf. We found this to be the case for all of the parameters but m_0 and sparticle masses that mostly depend on it, such as sleptons and squarks. For those quantities, choosing a prior $50 \text{ GeV} \leq m_0 \leq 2 \text{ TeV}$ cuts away a large region of parameter space that is not disfavoured by data, the so called “focus point region”. If the prior range is enlarged to $50 \text{ GeV} \leq m_0 \leq 4 \text{ TeV}$, then a considerable part of the focus point region is included in the analysis, even though it is still not possible to constrain the value of m_0 from above. With presently available data, any upper limit on m_0 is purely a consequence of the prior adopted. In the following we present results for the extended range with a prior region up to 4 TeV for $m_0, m_{1/2}$, and in the range $|A_0| \leq 7 \text{ TeV}$, $2 \leq \tan \beta \leq 62$. The prior range on the nuisance parameters does not influence the final results, since the SM parameters are rather tightly constrained by the data (summarized in the top section of Table 1).

For our analysis, from the CMSSM and SM parameters η we compute a series of derived observable quantities $f(\eta)$: the W gauge boson mass, the effective leptonic weak mixing angle $\sin^2 \theta_{\text{eff}}$, the anomalous magnetic moment of the muon, $a_\mu \equiv (g - 2)_\mu$, the branching ratios $BR(\bar{B} \rightarrow X_s \gamma)$ and $BR(B_s \rightarrow \mu^+ \mu^-)$, the cosmological neutralino relic abundance $\Omega_{\text{CDM}} h^2$ (by solving the Boltzmann equation numerically as in [12]), the light Higgs mass and the superpartner masses (computed with the package SOFT-SUSY v1.9 [13]). For all of those quantities, relevant measurements (summarized in the bottom section of Table 1) or experimental limits are included via the likelihood and

Nuisance parameter	Mean value		Uncertainty
	μ		experimental theoretical
M_t	172.7 GeV	2.9 GeV	N/A
$m_b(m_b)^{\overline{MS}}$	4.24 GeV	0.11 GeV	N/A
$\alpha_s(M_Z)^{\overline{MS}}$	0.1186	0.002	N/A
$1/\alpha_{em}(M_Z)^{\overline{MS}}$	127.958	0.048	N/A
Derived observable			
M_W	80.425 GeV	34 MeV	13 MeV
$\sin^2 \theta_{eff}$	0.23150	16×10^{-5}	25×10^{-5}
$\delta a_\mu^{USY} \times 10^{10}$	25.2	9.2	1
$BR(\bar{B} \rightarrow X_s \gamma) \times 10^4$	3.39	0.30	0.30
$\Omega_\chi h^2$	0.119	0.009	$0.1 \Omega_\chi h^2$

Table 1

Top section: experimental mean μ and standard deviation for the nuisance parameters used in the analysis. Bottom section: as above, but for derived observable quantities, including a theoretical uncertainty describing the imprecise mapping of CMSSM and SM parameters onto observable quantities. Notice that the value for the cosmological neutralino abundance $\Omega_\chi h^2$ stems from WMAP 1st year data combined with other cosmological observations.

used to constrain high posterior probability regions of the model. We assume that all of the cold dark matter is in the form of neutralinos. Furthermore, the likelihood is modified in such a way that it includes estimated theoretical uncertainties in the mapping from CMSSM and SM parameters to derived quantities, another major advantage of employing a Bayesian approach (see [8] for details). We then compute a spin-independent dark matter WIMP elastic scattering cross section on a free proton, σ_p^{SI} , including full supersymmetric contributions which have been derived by several groups [14,15,16,17,18], but we do not include current constraints in the likelihood, in view of the uncertainties in the structure of the Galactic halo (*e.g.*, existence of clumps of dark matter and therefore the value of the local halo mass density) as well as in the values of some hadronic matrix elements entering the computation of σ_p^{SI} . Our Bayesian approach allows to easily compute the posterior pdf for the cross section or any other derived variable. As we now discuss, our result for high-probability regions is highly suggestive of a possible detection by the next generation of direct dark matter searches.

3. Results for neutralino direct detection

In Fig. 1 we present the 2-dimensional posterior pdf for σ_p^{SI} and m_χ , with all other parameters marginalized over. For comparison, we also show current CDMS-II [19], Edelweiss-I [20] and UKDMC ZEPLIN-I [21] 90% CL upper limits, but we stress that this constraint has not been used in our analysis.

In Fig. 1 the biggest, banana-shaped region of high probability (68% regions delimited by the internal solid, blue curve) shows a well-defined anticorrelation between σ_p^{SI} and m_χ . It results from two allowed regions in the CMSSM

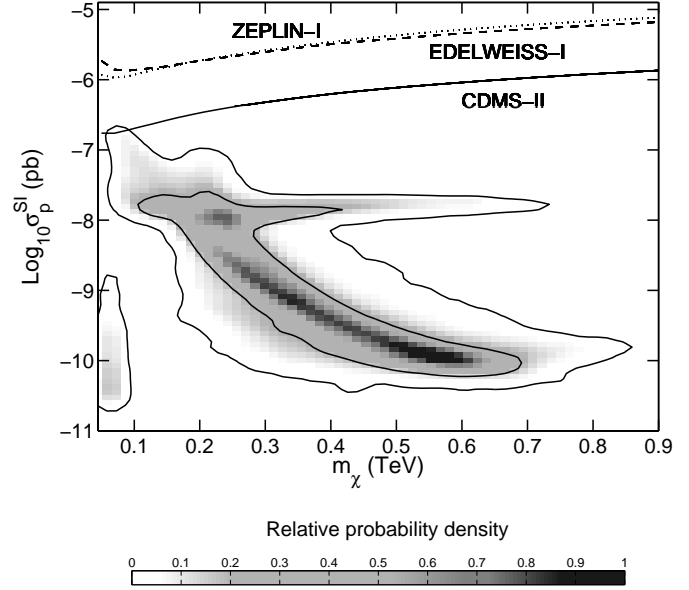


Fig. 1. The 2-dimensional probability density in the neutralino mass and spin-independent cross section plane in the CMSSM (all other parameters marginalized) with the contours containing 68% and 95% probability also marked. Current 90% experimental upper limits are also shown. A large fraction of the high-probability region lies just below current constraints and it will be probed by the next generation of dark matter searches, starting from the focus point region (horizontal region at $\sigma_p^{SI} \sim 10^{-8}$).

parameter space: the bulk and stau coannihilation region and from the A -resonance at large $\tan \beta$. This region covers roughly the range $10^{-10} \lesssim \sigma_p^{SI} \lesssim 10^{-8}$ pb and $200 \lesssim m_\chi \lesssim 700$ GeV. In both cases the dominant contribution to σ_p^{SI} comes from a heavy Higgs exchange. At small $m_\chi \lesssim 100$ GeV we notice a small vertical band of fairly low probability density ($\lesssim 0.2$) at small σ_p^{SI} , a region where the light Higgs resonance contribute to reducing $\Omega_\chi h^2$ at small $m_{1/2}$ to meet the WMAP measurement. It is interesting to notice that our Monte Carlo procedure is able to resolve such small features of parameter space, that are almost invariably missed by usual fixed-grid scans. This region would also disappear with a fair improvement in the lower bound on m_h . Finally, we can see a well pronounced region of high probability at fairly constant $\sigma_p^{SI} \sim 1.6 \times 10^{-8}$ pb for $m_\chi \lesssim 420$ GeV which at low m_χ partly overlaps with the previous region. At 95% this region extends up to $m_\chi \lesssim 720$ GeV for fairly constant σ_p^{SI} . This “high” σ_p^{SI} band results from the focus point region, basically independently of $\tan \beta$. This result has to be interpreted carefully, since there are large uncertainties associated with FP region, in particular with its location in the $(m_{1/2}, m_0)$ plane mentioned earlier. Despite those outstanding questions, we believe that it is safe to expect that the FP will be the first to be probed by dark matter search experiments.

After marginalizing over all other parameters, we obtain the following 1-dimensional regions encompassing 68% and 95% of the total probability (see Fig. 2):

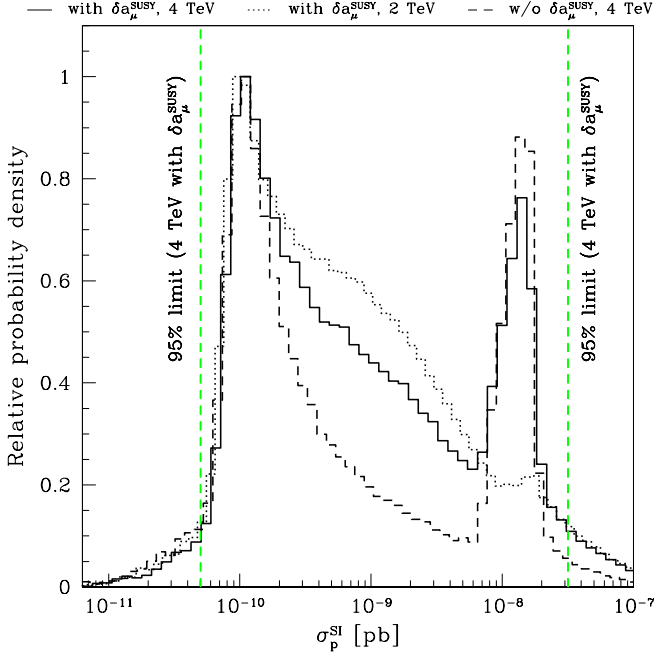


Fig. 2. The 1-dimensional probability distribution for the spin-independent neutralino scattering cross section in the CMSSM. The three curves explore the impact of different assumptions in the analysis: assuming a 4 TeV upper prior on m_0 (solid), a 2 TeV prior (dotted) or removing from the analysis the constrain from $g-2$ (dashed, for the 4 TeV prior case). The vertical, dashed lines delimit the region encompassing 95% probability for the 4 TeV prior and including $g-2$. The spike around $\sigma_p^{SI} \sim 10^{-8}$ corresponds to the focus point region at large m_0 . Future one-tonne detectors will reach down to $\sigma_p^{SI} \sim 10^{-10}$ and thus explore most of the 95% region.

$$\begin{aligned} 1.0 \times 10^{-10} \text{ pb} < \sigma_p^{SI} < 1.0 \times 10^{-8} \text{ pb} & \quad (68\% \text{ region}), \\ 0.5 \times 10^{-10} \text{ pb} < \sigma_p^{SI} < 3.2 \times 10^{-8} \text{ pb} & \quad (95\% \text{ region}). \end{aligned} \quad (4)$$

Currently running experiments (most notably CDMS-II but also Edelweiss-II and ZEPLIN-II) should be able to reach down to a few $\times 10^{-8}$ pb, on the edge of exploring this FP region. A future generation of “one-tonne” detectors is going to reach down to $\sigma_p^{SI} \gtrsim 10^{-10}$ pb, thus exploring almost the whole 68% region and much of the 95% interval as well.

This result for the pdf on σ_p^{SI} is rather robust with respect to a change in the prior range. The spike at $\sigma_p^{SI} \sim 10^{-8}$ disappears if one cuts away most of the focus point by imposing a prior $m_0 \leq 2$ TeV, but the 95% region is only slightly shifted to lower values. We have also considered the impact of removing from the analysis the constrain coming from $g-2$. We have found that in this case m_0 becomes essentially unconstrained, and this adds statistical weight to the focus point region. However, even in this case the high-probability range for σ_p^{SI} remains close to the values given in Eq. (4), shifting to $0.3 \times 10^{-10} \text{ pb} < \sigma_p^{SI} < 2.8 \times 10^{-8} \text{ pb}$ (95% probability region).

We notice that the high-probability regions as described above do not necessarily coincide with the best fitting

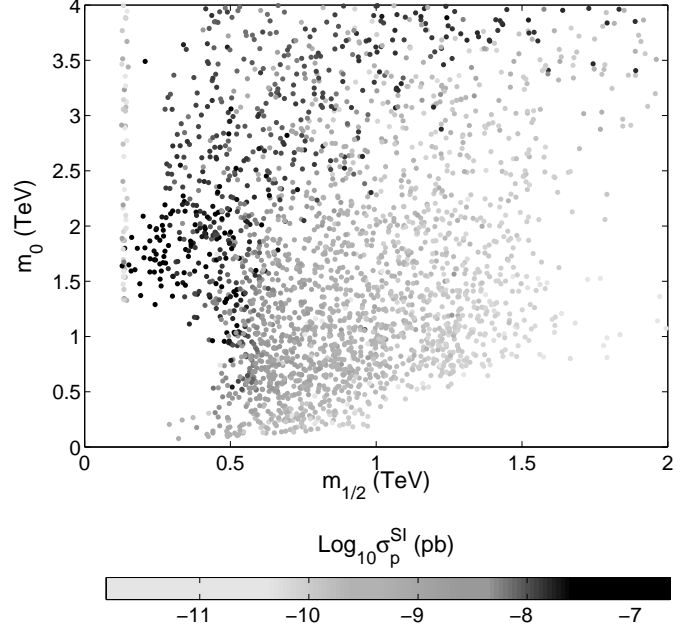


Fig. 3. Distribution of the values of σ_p^{SI} in the $(m_{1/2}, m_0)$ plane. The dots delimit the 95% confidence region in parameter space. Values down to $\sigma_p^{SI} \sim 10^{-8}$ (darker dots) will be among the first to be explored by currently running dark matter searches. This includes a large part of the focus point region at large m_0 .

points in parameter space if the pdf is strongly non-Gaussian, as in the present case. We refer the reader to [8] for a detailed description of the discrepancy and a discussion of its meaning in terms of probabilistic inference.

Finally, it is interesting to consider the complementarity between direct dark matter searches and the reach of future collider experiments, especially in view of the imminent start of operations at LHC. We plot in Fig. 3 the distribution of values of σ_p^{SI} in the plane $(m_{1/2}, m_0)$, where the points roughly cover the region encompassing 95% of probability. It is apparent that the largest values of the cross section ($\sigma_p^{SI} \gtrsim 10^{-8}$) are clustered in the region $200 \text{ GeV} \lesssim m_{1/2} \lesssim 500 \text{ GeV}$, covering values of m_0 all the way up to our prior limit of 4 TeV in the focus point region. As the currently running dark matter detectors start probing value down to $\sigma_p^{SI} \sim 10^{-8}$, they will begin exploring the focus point region of parameter space, which lies at large values of m_0 that are largely outside the reach of LHC searches. From our analysis a very promising synergy thus emerges between direct dark matter collider searches, that will soon begin to squeeze from different directions the current high-probability region of the CMSSM parameters space.

4. Conclusions

We have presented a detailed investigation of the prospects for dark matter detection in the framework of the CMSSM parameter using state-of-the-art Bayesian methods. The power and flexibility of the approach allows to probe many previously unexplored ranges of parameters and to fully incorporate the effects of remaining uncer-

tainties in relevant SM parameters and other theoretical uncertainties in computing mass spectra and observables.

We have shown that the WIMP dark matter direct detection elastic scattering cross section σ_p^{SI} presents a wide spread of values (below today's limits) at around $10^{-9\pm 1}$ pb and a strong anticorrelation with m_χ . In addition, a region at relatively large $\sigma_p^{SI} \simeq 1.6 \times 10^{-8}$ pb, and fairly independent of m_χ , appears to be a feature of the focus point region (despite large theoretical uncertainties) and will be the first to be tested in direct detection experiments.

Despite the remaining uncertainties arising from the local dark matter density profile and the large errors on nuclear form factors, it seems that a large fraction of the high-probability parameter space of neutralino dark matter in the CMSSM will be within reach of currently running upgraded dark matter detector, and most of it will be explored by future one-tonne detectors. We have highlighted the complementarity of these searches with direct SUSY searches at colliders and in particular showed that the focus point region, mostly outside the reach of the LHC, will be among the first to be probed by direct dark matter detection experiments. Those results are largely robust with respect to changes in the *a priori* allowed range for the parameters or to the exclusion of the anomalous magnetic moment of the muon measurement from the analysis.

Acknowledgements: R.T. is supported by the Royal Astronomical Society through the Sir Norman Lockyer Fellowship. R.Rda is supported by the program "Juan de la Cierva" of the Ministerio de Educación y Ciencia of Spain. R.Rda and R.T. would like to thank the European Network of Theoretical Astroparticle Physics ILIAS/N6 under contract number RII3-CT-2004-506222 for financial support.

References

- [1] G. L. Kane, C. F. Kolda, L. Roszkowski and J. D. Wells, *Study of constrained minimal supersymmetry*, *Phys. Rev.* **D49** (1994) 6173.
- [2] M. Drees and M. Nojiri, *The neutralino relic density in minimal $N=1$ supergravity*, *Phys. Rev.* **D47** (1993) 376.
- [3] H. Baer and M. Brhlik, *Cosmological relic density from minimal supergravity with implications for collider physics*, *Phys. Rev.* **D53** (1996) 597.
- [4] J. R. Ellis, T. Falk, K. A. Olive and M. Srednicki, *Calculations of neutralino-stau coannihilation channels and the cosmologically relevant region of MSSM parameter space*, *Astropart. Phys.* **13** (2000) 181 [Erratum-ibid. **15** (2001) 413]
- [5] J. R. Ellis, T. Falk, G. Ganis, K. A. Olive and M. Srednicki, *The CMSSM parameter space at large $\tan \beta$* , *Phys. Lett.* **B510** (2001) 236.
- [6] T. Nihei, L. Roszkowski and R. Ruiz de Austri, *New Cosmological and Experimental Constraints on the CMSSM*, *JHEP* **0108** (2001) 024
- [7] A. Lahanas and V. Spanos, *Implications of the pseudo-scalar Higgs boson in determining the neutralino dark matter*, *Euro. Phys. Journ.* **C23** (2002) 185.
- [8] R. Ruiz de Austri, R. Trotta and L. Roszkowski, *A Markov Chain Monte Carlo analysis of the CMSSM* (2006) *JHEP* **05** (2006) 002.
- [9] E. A. Baltz and P. Gondolo, *Markov chain monte carlo exploration of minimal supergravity with implications for dark matter*, *JHEP* **0410** (2004) 052.
- [10] B. C. Allanach and C. G. Lester, *Multi-dimensional MSUGRA likelihood maps*, arXiv:hep-ph/0507283.
- [11] B. C. Allanach, *Naturalness priors and fits to the constrained minimal supersymmetric standard model*, arXiv:hep-ph/0601089.
- [12] P. Gondolo, J. Edsjo, P. Ullio, L. Bergstrom, M. Schelk and E. A. Baltz, *DARKSUSY: computing supersymmetric dark matter properties numerically*, <http://www.physto.se/edsjo/darksusy/>.
- [13] B. C. Allanach, *SOFTSUSY: a C++ program for calculating supersymmetric spectra*, *Comput. Phys. Commun.* **C143** (2002) 305.
- [14] M. Drees and M. Nojiri, *Neutralino-nucleon scattering revised*, *Phys. Rev.* **D48** (1993) 3483.
- [15] For a review, see, e.g., G. Jungman, M. Kamionkowski and K. Griest, *Supersymmetric dark matter*, *Phys. Rep.* **267** (1996) 195.
- [16] H. Baer and M. Brhlik, *Neutralino dark matter in minimal supergravity: direct detection versus collider searches*, *Phys. Rev.* **D57** (1998) 567.
- [17] J. Ellis, A. Ferstl and K. A. Olive, *Reevaluation of the elastic scattering of supersymmetric dark matter*, *Phys. Lett.* **B481** (2000) 304.
- [18] Y. G. Kim, T. Nihei, L. Roszkowski and R. Ruiz de Austri, *Upper and lower limits on neutralino WIMP mass and spin-independent scattering cross section, and impact of new $(g-2)_\mu$ measurement*, *JHEP* **0212** (2002) 034, .
- [19] D. S. Akerib, et al., [CDMS Collaboration], *First results from the cryogenic dark matter search in the Soudan underground lab.*, *Phys. Rev. Lett.* **B93** (2004) 211301.
- [20] V. Sanglard et al.[EDELWEISS Collaboration], *Final results of the EDELWEISS-I dark matter search with cryogenic heat-and-ionization Ge detectors*, *Phys. Rev.* **D71** (2005) 122002.
- [21] G. J. Alner et al.[UK Dark Matter Collaboration], *First limits on nuclear recoil events from the ZEPLIN-I galactic dark matter detector*, *Astropart. Phys.* **23** (2005) 444.